Available online at www.sciencedirect.com
SCIENCE DIRECT
Surface Science 600 (2006) 514–526
SURFACE SCIENCE
www.elsevier.com/locate/susc

Isomeric effects on room-temperature chemisorption and thermal evolution of *iso*-, *cis*- and *trans*-dichloroethylene on Si(1 1 1)7 × 7

Zhenhua He, Q. Li, K.T. Leung *

Department of Chemistry, University of Waterloo, 200 University Ave West, Waterloo, Ont., Canada N2L 3G1

Received 14 February 2005; accepted for publication 8 November 2005
Available online 7 December 2005

Abstract

The room-temperature adsorption and thermal evolution of *iso*-, *cis*- and *trans*-dichloroethylene (DCE) on Si(1 1 1)7 × 7 have been studied by vibrational electron energy loss spectroscopy and thermal desorption spectrometry (TDS). The presence of the Si–Cl stretch at 510 cm^{-1} suggests that, upon adsorption, all three isomers dissociate via C–Cl bond breakage on the 7 × 7 surface to form mono-σ bonded chlorovinyl (HĊ=CHCl or ClĊ=CH_2), which could, in the case of *iso*-DCE, further dechlorinate to vinylidene (:C=CH_2) upon insertion into the back-bond. The higher saturation exposure for the Si–Cl stretch at 510 cm^{-1} observed for *cis*- and *trans*-DCE than *iso*-DCE suggests that Cl dissociation via the =CHCl group in the *cis* and *trans* isomers is less readily than the =CCl_2 group in *iso*-DCE. Our TDS data show remarkable similarities in both molecular desorption near 360 K and thermal evolution of the respective adstructures for all three isomers on Si(1 1 1)7 × 7. In particular, upon annealing to 450 K, the mono-σ bonded chlorovinyl adspecies is found to further dechlorinate to either vinylene (HĊ=ĊH) di-σ bonded to the Si surface or acetylene to be released from the surface. Above 580 K, vinylene could also become gaseous acetylene or undergo H abstraction to produce hydrocarbon or SiC fragments. All three DCE isomers also exhibit TDS features attributable to an etching product $SiCl_2$ at 800–950 K and recombinative desorption products HCl at 700–900 K and H_2 at 650–820 K. The stronger Cl-derived TDS signals and Si–Cl stretch at 510 cm^{-1} over 450–820 K for *trans*-DCE than those for *cis*-DCE indicate stronger dechlorination for *trans*-DCE than *cis*-DCE, which could be due to less steric hindrance resulting from the formation of the chlorovinyl adspecies for *trans*-DCE during the initial adsorption/dechlorination process. Finally, our density functional calculations qualitatively support the thermodynamic feasibility and relative stabilities of the proposed adstructures involving chlorovinyl, vinylidene, and vinylene adspecies.

Keywords: Chemisorption; Dechlorination; Chloroethylenes; Vinylidene; Vinylene; Si(1 1 1)7 × 7; Electron energy loss spectroscopy; Thermal desorption spectrometry

1. Introduction

The interactions of chlorinated hydrocarbons and their derivatives with silicon surfaces are of practical interest to the semiconductor industry due to their important role as common industrial chemicals for microelectronic device fabrication and processing [1–3]. For example, *trans*-dichloroethylene (*trans*-DCE) and trichloroethylene (TCE) have been used as a Cl source to reduce metal contamination during Si oxidation [4,5]. Chlorinated hydrocarbons also attract a lot of attention as potential precursors in photochemical etching of semiconductor surfaces [6–9]. The combination of the simplest unsaturated hydrocarbons (ethylene) with chlorine provides an important family of chloroethylenes with a wide range of structural possibilities and chemical properties that are of fundamental interest to organosilicon chemistry. Despite a considerable amount of work on catalytic degradation

* Corresponding author. Tel.: +1 5198884567x5826; fax: +1 5197460435.
E-mail address: tong@uwaterloo.ca (K.T. Leung).

0039-6028/$ - see front matter © 2005 Elsevier B.V. All rights reserved.
doi:10.1016/j.susc.2005.11.003

of chlorinated ethylenes on metal surfaces [10–16], the interactions of these compounds with silicon remain largely unexplored. The studies on metal surfaces focus primarily on multilayer (physi-)adsorption near liquid-nitrogen temperature and chemisorption behaviour upon annealing toward room temperature (RT). In particular, using vibrational electron energy loss spectroscopy (EELS) and thermal desorption spectrometry (TDS), Grassian and Pimental showed that *cis*- and *trans*-DCE form di-σ bonds with Pt(1 1 1) in staggered, alkane-like geometries upon monolayer and submonolayer adsorption at 110 K, and undergo dechlorination above 200 K producing a vinylene or ethene-1,2-diyl (HĊ=ĊH) adspecies[1] [11]. Later, Cassuto et al. concluded from their XPS study that on Pt(1 1 1) and Pt(1 1 0) DCE (*cis*, *trans* and *iso* isomers), TCE and perchloroethylene (PCE) are weakly bonded at 95 K (with the molecular plane parallel to the surface) and they could be desorbed molecularly above 120–130 K [16]. Furthermore, Yang et al. studied the chemical bonding and reactions of a series of chloroethylenes [including monochloroethylene (MCE), *cis*- and *trans*-DCE, and TCE] on Cu(1 0 0) using TDS and near-edge X-ray absorption fine structure technique [12], and they suggested that molecular adsorption of these chloroethylenes at 95 K could involve π-bonding interaction with the Cu surface. With the exception of MCE that was found to desorb molecularly upon annealing, enhanced dechlorination with increasing Cl content in the adsorbate was observed for the heavier chloroethylenes, and the resulting dissociated hydrocarbon product (acetylene) could lead to benzene evolution in the case of *cis*- and *trans*-DCE, and TCE [12]. On Cu(1 1 0), however, Jugnet et al. proposed, on the basis of their EELS data, a di-σ bonded adstructure for *trans*-DCE chemisorbed at 135 K, which could evolve into acetylene-like adspecies by C–Cl bond cleavage upon annealing to ~200 K and to benzene at a higher temperature [13]. The formation of benzene could also be observed by direct adsorption of *trans*-DCE at RT [13].

Unlike metal surfaces, low-Miller-index surfaces of silicon offer unique covalent bonding possibilities for surface reconstruction and chemistry involving the directional surface dangling bonds. The interactions of simple unsaturated (π-bonded) hydrocarbons such as ethylene and acetylene on Si(1 1 1)7 × 7 and Si(1 0 0)2 × 1 with one and two directional dangling bonds per surface Si atom, respectively, have been studied extensively [17–21]. Given that the physical structures of chloroethylenes could be closely matched to the separations among different dangling-bond sites on the 7 × 7 or 2 × 1 reconstructed surfaces, the chloroethylenes series provides an ideal platform for studying various fundamental chemical effects, including the differences in the chemisorption and thermal evolution behaviours produced by different geometrical isomers of DCE or by the heavier homologs with increasing Cl content. Furthermore, chloroethylenes consist only of three basic bonding components (C=C, C–H, and C–Cl), the vibrational spectra of which have been well characterized in the gas or liquid phase, making a comparative study of their corresponding surface vibrational spectra manageable. Of special interests are the possible surface chemical processes involving these basic bonding components upon chemisorption, which include π-bond saturation, dehalogenation, surface etching and polymerization.

Recently, our group has initiated a series of systematic studies of the surface chemical processes of chloroethylenes on Si(1 1 1) and Si(1 0 0) surfaces by using TDS, vibrational EELS [22], and X-ray photoelectron spectroscopy (XPS) [23]. The effects of increasing chlorine content in the chloroethylene homologs on their surface chemistry on Si(1 1 1)7 × 7 have been demonstrated in our recent studies on ethylene, MCE, and *iso*-DCE [24] and on PCE and TCE [25], which focus on the identification of novel adstructures and their thermal evolution. We now present a comparative study on the RT adsorption properties of the three geometrical isomers of DCE (*cis* and *trans* 1,2-DCE, and *iso* or 1,1-DCE) on Si(1 1 1)7 × 7 and compare the thermal evolution behaviour of the resulting adspecies by using vibrational EELS and TDS.

2. Experimental details

The experimental setup and procedure used in the present work have been described in detail elsewhere [26]. Briefly, the experiments were conducted in a home-built ultrahigh vacuum system with a base pressure better than 5×10^{-11} Torr. All of the EELS measurements were made with the sample held at RT under specular reflection scattering condition of 45° from the surface normal. A routine energy resolution of 12–17 meV (or 97–136 cm^{-1}) full-width at half-maximum with a typical count rate of 100,000 counts/s for the elastic peak could be achieved with our spectrometer operated at 5 eV impact energy. It should be noted that the calibration and tuning of the EELS spectrometer typically limit the reproducibility of the measured peak positions to ±2 meV (or ±16 cm^{-1}) in the present work. The TDS experiments were obtained by using a differentially pumped quadrupole mass spectrometer (QMS) to monitor the ion fragments, along with a home-built programmable proportional–integral–differential temperature controller to provide a linear heating rate of 1 K s^{-1}. The TDS data have been smoothed by adjacent averaging and the respective monotonically increasing backgrounds with increasing temperature have also been removed in order to more clearly identify the desorption features. The absolute accuracy for the temperatures of desorption features was found to be ±10 K. The Si(1 1 1) sample (p-type boron-doped, 50 Ω cm, 8 × 6 mm^2, 0.5 mm thick) with a stated purity of 99.999% was purchased from Virginia Semiconductor Inc. The sample was mechanically fastened to a Ta sample plate with 0.25-mm-diameter Ta wires and could be annealed by electron bombardment from a heated

[1] We use "·" or "-" to denote an unpaired electron available for bonding with a substrate atom.

tungsten filament at the backside of the sample. The Si(1 1 1) sample was cleaned by a standard procedure involving repeated cycles of Ar^+ sputtering and annealing to 1200 K until a sharp 7×7 LEED pattern was observed. The cleanliness of the 7×7 surface was further verified in situ by the lack of any detectable vibrational EELS feature attributable to unwanted contaminants, particularly the Si–C stretching mode at 800–850 cm^{-1}. The liquid samples *iso*-DCE (99% purity), *cis*-DCE (98% purity), and *trans*-DCE (98% purity) were purchased from Sigma-Aldrich and used (without further purification) after appropriate degassing by repeated freeze–pump–thaw cycles. All the exposures were conducted at a typical pressure of 1×10^{-6} Torr as monitored by an uncalibrated ionization gauge by using a variable leak valve.

3. Results and discussion

3.1. Room-temperature adsorption of cis- and trans-DCE on Si(1 1 1)7 × 7

Fig. 1 compares the vibrational EELS spectra for saturation exposures of TCE, *iso*-DCE, *cis*-DCE and *trans*-DCE on Si(1 1 1)7×7 at RT. To facilitate the spectral assignments, the surface vibrational EELS data obtained in the present work are compared with the corresponding infrared and Raman spectroscopic data of chloroethylenes obtained in the gas or liquid phase [27]. Evidently, all four chloroethylenes exhibit a prominent feature at 2980 cm^{-1} characteristic of the C–H stretching mode [27], a well-defined feature at 510 cm^{-1} attributable to the Si–Cl stretching mode [28,29], and weak and broad bands in the 600–1800 cm^{-1} region. In contrast to the C–H stretching mode found at 2900 cm^{-1} for ethylene, which is believed to be di-σ bonded to the 7×7 surface (with C sp^3 hybridization) as an ethane-1,2-diyl adspecies [24], the C–H stretching mode found at the higher frequency (2980 cm^{-1}) indicates C sp^2 hybridization, suggesting that [2 + 2] cycloaddition does not play a major role. Furthermore, the presence of the Si–Cl feature at 510 cm^{-1} indicates dechlorination and the corresponding peak intensity can be used to indicate the relative Cl surface moiety. The dissociation of Cl from all four chloroethylenes is also supported by the evolution of the sharp 7×7 LEED pattern of the clean Si(1 1 1) surface to a diffuse 7×7 and eventually 1×1 pattern upon a saturation exposure. On the other hand, the lack of a Si–H stretching mode commonly found near 2100 cm^{-1} [30] suggests that hydrogen abstraction of chloroethylenes does not play a prominent role on Si(1 1 1)7×7. The mid-frequency regions for TCE (Fig. 1a) and *iso*-DCE (Fig. 1b) have been previously assigned in our recent work [24,25]. Briefly, the well-defined features observed at 1510 cm^{-1}, 1150 cm^{-1}, and 820 cm^{-1} for TCE (Fig. 1a) can be attributed to C=C stretching, CH in-plane bending, and C–Cl stretching modes, respectively. Similarly, the weak features at 1510 cm^{-1}, 1360 cm^{-1} and 1050 cm^{-1} found for *iso*-DCE (Fig. 1b) can be assigned to C=C stretching, CH_2 scissoring, and CH_2 rocking modes, respectively. In the case of *cis*-DCE and *trans*-DCE, the weak broad band at 1000–1700 cm^{-1} and the weak shoulder near 750 cm^{-1} can be attributed to CH in-plane and out-of-plane bending modes and to C–Cl stretching mode, respectively [27].

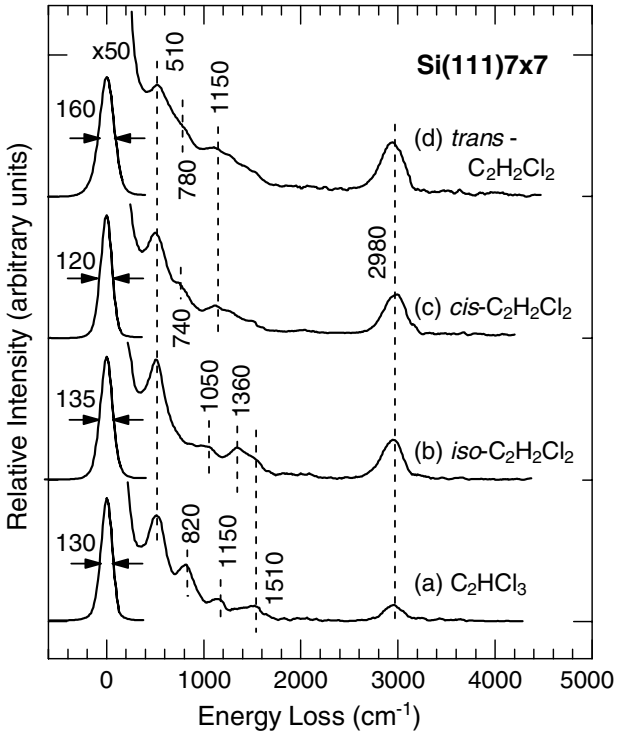

Fig. 1. Vibrational electron energy loss spectra for (a) 100 L of trichloroethylene, (b) 100 L of *iso*-dichloroethylene, (c) 1000 L of *cis*-dichloroethylene, and (d) 1000 L of *trans*-dichloroethylene exposed to Si(1 1 1)7×7 at room temperature.

The generally similar EELS spectra for all four chloroethylenes (Fig. 1) suggest similarities in their adsorption structures at RT. In particular, the vibrational spectra for *cis*-DCE (Fig. 1c) and *trans*-DCE (Fig. 1d) on the 7×7 surface are nearly identical to each other, while minor differences are found in the mid-frequency regions among these two isomers and *iso*-DCE and TCE. In order to illustrate the similarities in the RT adsorption and thermal evolution behaviours of these chloroethylene molecules on the 7×7 surface, we show in Fig. 2 schematic diagrams of plausible adstructures at different temperatures for the three isomers of DCE. A similar schematic diagram for TCE has been given in our recent work [25]. The C–H stretching mode at a relatively high frequency (2980 cm^{-1}, corresponding to C sp^2 hybridization) along with the presence of the weak C=C stretch at 1510 cm^{-1} strongly suggest a mono-σ bonded 1-chlorovinyl adspecies (Cl$\dot{C}$=CH_2, Structure I, Fig. 2a) for *iso*-DCE [24] and 2-chlorovinyl adspecies (H$\dot{C}$=CHCl) for *cis*-DCE (Structure IV, Fig. 2b) and *trans*-DCE (Structure V, Fig. 2b). This picture is consistent with the presence of the Si–Cl stretch at 510 cm^{-1} as a result of dechlorination upon adsorption.

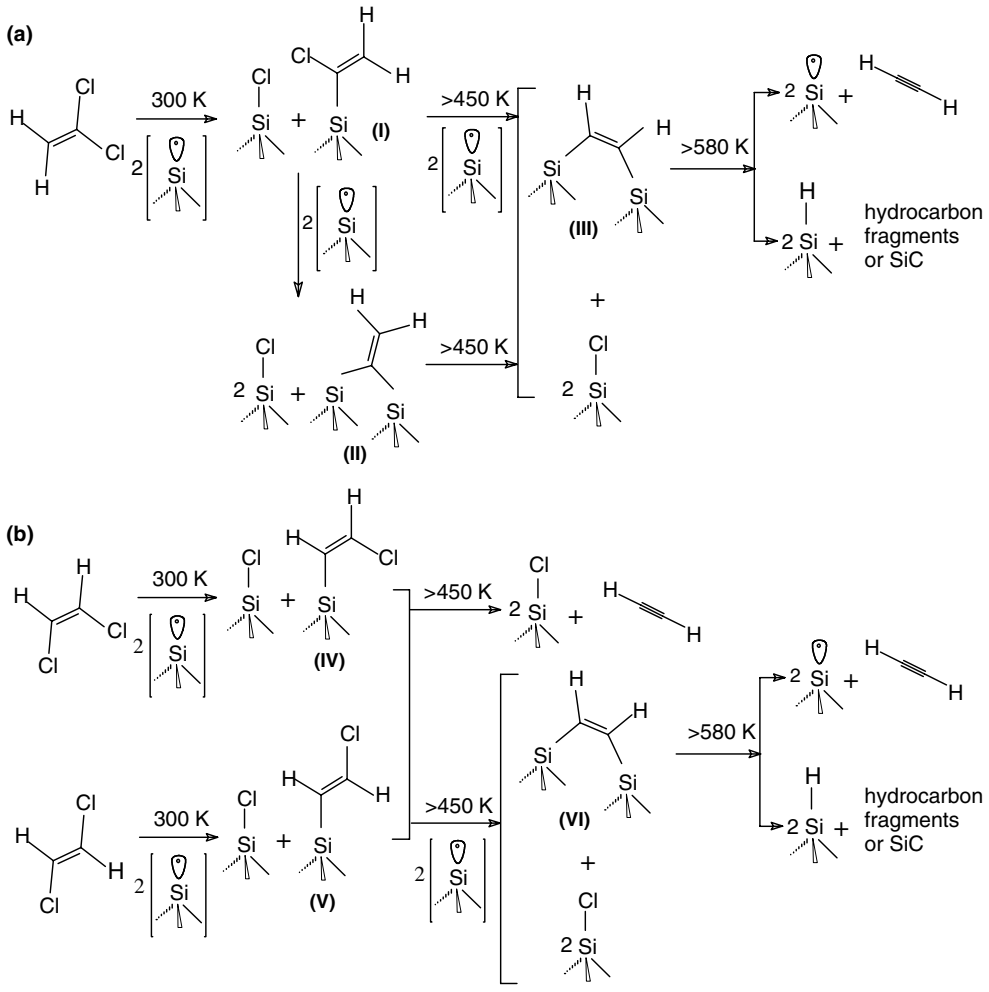

Fig. 2. Schematic diagrams of plausible adsorption structures and thermal evolution products for saturation exposures of (a) *iso*-dichloroethylene, and (b) *cis*- and *trans*-dichloroethylene to Si(1 1 1)7 × 7 at room temperature.

In the case of *iso*-DCE [24] (and TCE [25]), double dechlorination could also lead to di-σ bonded vinylidene (Structure II, Fig. 2a). The preference for Cl dissociation over H abstraction (as evidenced by the lack of Si–H peak near 2100 cm^{-1} [30] found for all four chloroethylenes shown in Fig. 1) is in accord with the stronger bond strength of Si–Cl (377 kJ mol^{-1}) relative to that of C–Cl (339 kJ mol^{-1}), and the stronger C–H bond strength (414 kJ mol^{-1}) relative to the Si–H bond strength (314 kJ mol^{-1}) [1,31,32]. Discernible differences between the EELS spectrum of *iso*-DCE and those of *cis*- and *trans*-DCE can be observed in the mid-frequency region. In particular, the absence of a CH_2 group in *cis*- and *trans*-DCE (and in their corresponding adstructures on the 7 × 7 surface) is clearly reflected by the weaker EELS intensity at 1360 cm^{-1} (Fig. 1c and d), attributable to the CH_2 scissoring mode, when compared to their *iso* homolog (Fig. 1b). Furthermore, the discernible C–Cl stretching mode near 750 cm^{-1} found for *cis*-DCE (Fig. 1c) and *trans*-DCE (Fig. 1d) supports our earlier hypothesis that mono-σ bonded 2-chlorovinyl adspecies (Structures IV and V, Fig. 2b) are preferred, in marked contrast to the lack of intensity for this feature in *iso*-DCE (Fig. 1b), which favours the di-σ bonded vinylidene adstructure (Structure II, Fig. 2a). The weaker intensity of Si–Cl stretch (at 510 cm^{-1}) relative to that of C–H stretch (at 2980 cm^{-1}) for *cis*- and *trans*-DCE than the corresponding intensity ratio for *iso*-DCE further supports the 2-chlorovinyl adstructures resulting from single dechlorination in the *cis*- and *trans*-DCE, instead of vinylidene produced by double dechlorination in *iso*-DCE.

Vibrational EELS spectra for the three DCE isomers and TCE have also been obtained as a function of the exposure. To illustrate the exposure dependence on the RT adsorption, we compare in Fig. 3 the intensities of the C–H stretching modes (at 2980 cm^{-1}) of the four chloroethylenes relative to the respective elastic peaks as a function of exposure. Evidently, the saturation exposures for *cis*- and *trans*-DCE on the 7 × 7 surface (∼200 L) are considerably larger than that for *iso*-DCE (∼10 L) and that for TCE (∼20 L). The C–H stretching mode could originate from adstructures resulting from not only dissociative adsorption as those shown in Fig. 2 but also molecular adsorption. Our recent TDS studies on *iso*-DCE [24] (and TCE [25]) suggest that these molecular adsorption species

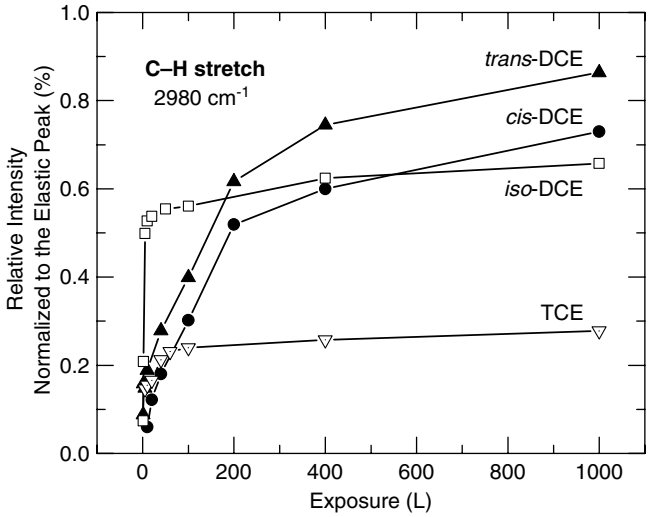

Fig. 3. Exposure dependence of the relative intensities of the C–H stretch normalized to the respective elastic peaks for *iso*-, *cis*- and *trans*-dichloroethylene (DCE) and trichloroethylene (TCE) on Si(1 1 1)7 × 7 at room temperature.

could occur as a result of weak inductive bonding and therefore should exhibit relatively low desorption temperature (no greater than 400 K). However, the lack of any significant change in the spectral intensity of the C–H stretching mode upon annealing the sample to 450 K indicates that these molecular adstructures do not play a substantial role in the initial adsorption at RT [24]. The observed spectral intensity of the C–H stretch could therefore be attributed predominantly to the more stable dissociative adstructures (such as the chlorovinyl adspecies) shown in Fig. 2. It should be noted that the presence of molecular adstructure due to [2 + 2] cycloaddition as in the case of MCE and ethylene [24] is also not likely because the location of the C–H stretch supports C sp^2 and not sp^3 hybridization. As we show in the next section, similar thermal evolution patterns can also be observed for the spectral intensity of the C–H stretching mode in *cis*- and *trans*-DCE. The observed lower saturation exposure for *iso*-DCE than the *cis* and *trans* isomers therefore suggests that Cl dissociation via the $=CCl_2$ group occurs more readily than the =CHCl group. This result is consistent with the observation that C–Cl bond cleavage is more facile in the $>CCl_2$ group than the >CHCl group found in the adsorption of multiply chlorinated hydrocarbons on Cu(1 0 0) by Yang et al. [33]. In addition, the relative intensities of the C–H stretch for the DCE isomers at saturation coverages are found to be similar to one other and are more than double that for TCE (Fig. 3), which is consistent with the respective H stoichiometry in the corresponding adstructures and that dissociative adsorption does not involve hydrogen abstraction.

It should be noted that we also collected EELS spectra for our sample pre- and post-exposed with O_2 (not shown). In particular, no EELS features attributable to *cis*- and *trans*-DCE are observed for an oxidized Si(1 1 1) surface exposed to 200 L of DCE. Similarly, the EELS spectrum for a saturated exposure of *cis*- or *trans*-DCE to Si(1 1 1) is unchanged by post-exposure with 200 L of O_2, and no Si–O–Si related feature is found. These results show that dangling bonds are required for the initial adsorption of O_2 or *cis*- and *trans*-DCE, and exposure of any of these adsorbates (like *iso*-DCE) produces the effect of passivating the surface. These results are also consistent with the conversion of the 7 × 7 LEED pattern for the clean surface to a 1 × 1 pattern for the surface exposed with *cis*-DCE or *trans*-DCE.

3.2. Thermal evolution of cis- and trans-DCE on Si(1 1 1)7 × 7

Figs. 4 and 5 show respectively the TDS profiles of selected mass fragments for 1000 L of *cis*-DCE and *trans*-DCE exposed to Si(1 1 1)7 × 7 at RT. With the exception of minor changes in the intensity ratios of the desorption features, the TDS profiles for the two adsorbates are very similar to each other. In particular, for both *cis*-DCE (Fig. 4) and *trans*-DCE (Fig. 5), a common desorption feature for mass 98 ($C_2H_2{}^{35}Cl^{37}Cl^+$, Curves f), mass 96 ($C_2H_2{}^{35}Cl_2^+$, corresponding to the parent mass, Curves e) and mass 63 ($C_2H_2{}^{37}Cl^+$, Curves d) with a desorption maximum at 360 K can be observed. These peaks at 360 K follow the same intensity ratios for both *cis*- and *trans*-DCE. Since these intensity ratios are found to be in good accord

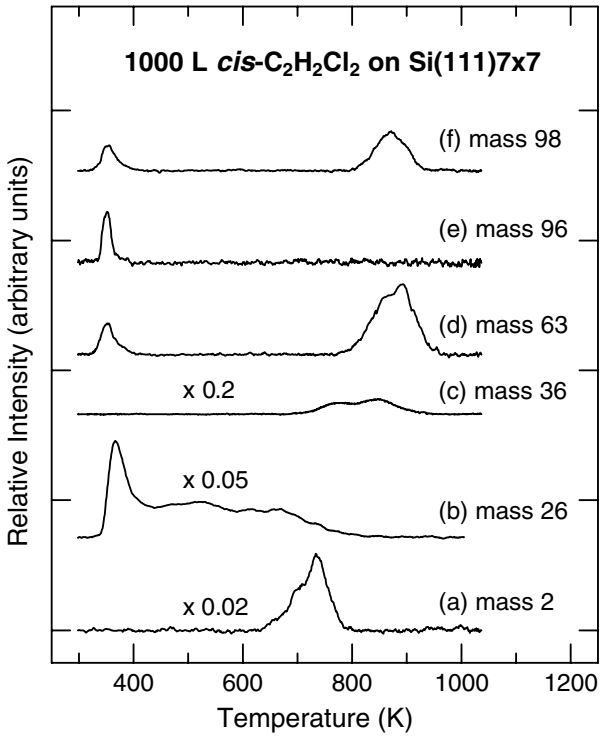

Fig. 4. Thermal desorption profiles of (a) mass 2 (H_2^+), (b) mass 26 ($C_2H_2^+$), (c) mass 36 (HCl^+), (d) mass 63 ($C_2H_2{}^{37}Cl^+$ or $Si^{35}Cl^+$), (e) mass 96 ($C_2H_2{}^{35}Cl_2^+$), and (f) mass 98 ($C_2H_2{}^{35}Cl^{37}Cl^+$ or $Si^{35}Cl_2^+$) for 1000 L of *cis*-dichloroethylene exposed to Si(1 0 0)7 × 7 at room temperature.

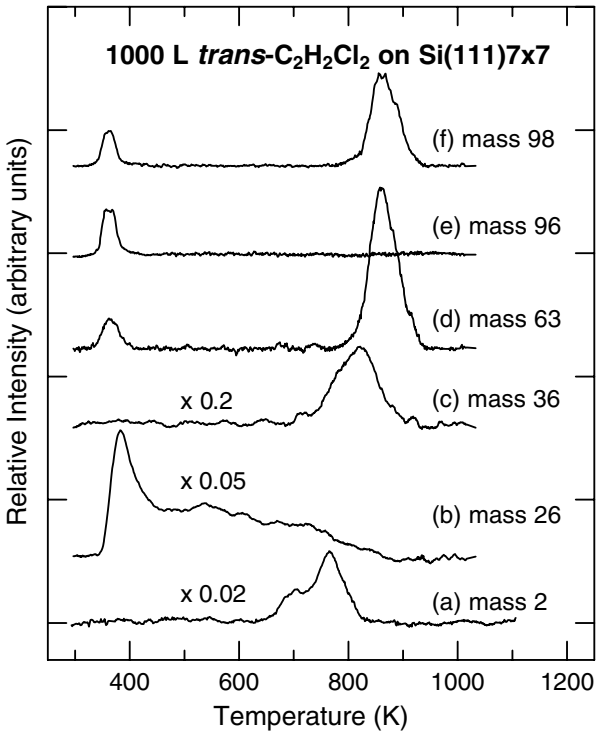

Fig. 5. Thermal desorption profiles of (a) mass 2 (H_2^+), (b) mass 26 ($C_2H_2^+$), (c) mass 36 (HCl^+), (d) mass 63 ($C_2H_2{}^{37}Cl^+$ or $Si^{35}Cl^+$), (e) mass 96 ($C_2H_2{}^{35}Cl_2^+$), and (f) mass 98 ($C_2H_2{}^{35}Cl^{37}Cl^+$ or $Si^{35}Cl_2^+$) for 1000 L of *trans*-dichloroethylene exposed to Si(1 0 0)7 × 7 at room temperature.

with the respective ratios in the cracking patterns of *cis*- and *trans*-DCE [34], the detected mass fragments could be attributed to dissociation of molecularly desorbed *cis*- and *trans*-DCE in the ionizer of the QMS. The low temperature found for the desorption maxima of the parent masses of *cis*-DCE (Fig. 4f and e) and *trans*-DCE (Fig. 5f and e) suggests that the molecularly desorbed species are from as-deposited (intact) molecules and not from recombinative desorption of adsorbed dissociated fragments, which would require a higher desorption temperature. One possible bonding arrangement may involve dative covalent bonding (between Cl atoms and the substrate Si atoms) as a result of the inductive effect of the Cl atoms. However, the bonding structures for such type of molecular adspecies of *cis*- and *trans*-DCE remain unclear. It should be noted that careful efforts have been made to assure that the desorbed species indeed originated from the Si sample and not the sample holder. In particular, the front face of the sample was positioned as close as possible (within 1 mm) to the entrance of the differentially pumped housing of the QMS during the TDS experiments, in order to effectively minimize the background and the amount of desorbed species originating from the surroundings [26]. Moreover, TDS experiments for *cis*- and *trans*-DCE on a Ni(1 1 0) surface performed using the same sample holder setup have not revealed the same desorption products, which further supports that the desorbed species indeed come from the Si sample and not the sample holder.

In addition to these low-temperature molecular desorption features found for mass 98, mass 96 and mass 63, an intense desorption peak of mass 26 is also observed at 380 K for both *cis*-DCE (Fig. 4b) and *trans*-DCE (Fig. 5b). The observed mass 26 desorption intensity relative to the parent mass (mass 96) is found to be considerably greater than that found in the respective gas-phase cracking patterns of *cis*- and *trans*-DCE, confirming that the observed feature is likely due to desorption of acetylene [34]. A possible mechanism for the apparently enhanced production of acetylene is the double dechlorination of the inductively bonded *cis*-or *trans*-DCE, in which two Cl atoms are transferred from the molecularly bonded *cis*-or *trans*-DCE to the substrate releasing the acetylene. This mechanism is generally consistent with the propensity of *cis*- and *trans*-DCE to dechlorinate on the Si surface, likely because of the stronger bond strength of Si–Cl (377 kJ mol^{-1}) than that of C–Cl (339 kJ mol^{-1}) [1,31,32]. In contrast, this mass 26 TDS feature at 380 K is not observed in the case of *iso*-DCE on Si(1 1 1)7 × 7 [24]. The lack of this low-temperature mass 26 TDS feature for *iso*-DCE could be attributed to the presence of a production pathway for vinylidene (Fig. 2a), which provides a strong adsorption structure that in turn prevents the formation of acetylene at this temperature [24].

For both *cis*-DCE (Fig. 4) and *trans*-DCE (Fig. 5), the respective TDS profiles of mass 98 (Curves f) and mass 63 (Curves d) also exhibit a broad feature located at 800–950 K, which could be attributed to the desorption of $SiCl_2^+$ and $SiCl^+$, respectively. Earlier chemisorption studies of $SiCl_4$ and SiH_2Cl_2 on Si(1 0 0) and Si(1 1 1) surfaces show that these higher-temperature TDS features may correspond to disproportionation of two monochloride species [35]. The nearly identical profiles of these higher-temperature features of mass 98 and mass 63 (with an intensity ratio of 1.8 for mass 63 to mass 98) indicate that they originate from the same desorption product. Because $SiCl_2^+$ (mass 98) and $SiCl^+$ (mass 63) are found to be in comparable amounts from electron impact studies of gaseous $SiCl_2^+$ [36,37], the parent desorption species is likely $SiCl_2$. We have also monitored mass 133, corresponding to $SiCl_3^+$ of the heavier etching product $SiCl_4$, but found no desorption feature, which therefore further confirms $SiCl_2$ as the main etching product. Furthermore, a broad desorption band of mass 36 (HCl^+, Curves c) [and of mass 35 (Cl^+, not shown)] at 700–900 K is also observed for both *cis*-DCE (Fig. 4) and *trans*-DCE (Fig. 5), which indicates recombinative desorption of HCl upon annealing to these temperatures. Like mass 98 and mass 63, the band intensity of mass 36 (Fig. 4c) relative to the parent mass (mass 96) for *cis*-DCE is considerably lower than that for *trans*-DCE. Assuming the degree of molecular desorption is similar for both *cis*- and *trans*-DCE, the differences in the Cl-derived TDS signals are consistent with the stronger dechlorination observed for *trans*-DCE than *cis*-DCE, likely due to less steric hindrance (and therefore greater adsorption) resulting from the formation of 1-chlorovinyl

adspecies in the *trans*-DCE case (Structure V, Fig. 2b). Stronger dechlorination for *trans*-DCE than *cis*-DCE is also evident from their respective mass 98 and mass 63 profiles. In particular, the intensity ratios of the higher-temperature feature at 800–950 K (corresponding to $SiCl_2^+$) to the lower-temperature feature near 380 K (corresponding to molecular desorption) for both mass 98 and mass 63 for *trans*-DCE are found to be 13 while those for *cis*-DCE are estimated to be 6. This large difference could only be due to stronger chlorination in *trans*-DCE than in *cis*-DCE and not to any run-to-run variations in our TDS experiments. Moreover, both *cis*-DCE and *trans*-DCE also exhibit an intense broad TDS feature of mass 2 (H_2^+) at 650–820 K (with desorption maximum near 750 K), in good accord with the recombinative desorption of H_2 (with desorption maxima commonly observed at 650–710 K for dihydrides and at 770–810 K for monohydrides [38,39]). The presence of the mass 2 TDS features confirms H abstraction and the formation of hydrocarbon fragments upon annealing the sample to these higher temperatures. In addition to the intense peak at 380 K, desorption intensity over a wide temperature range of 450–820 K can also be observed in the TDS profiles of mass 26 (Curves b) for both *cis*-DCE (Fig. 4) and *trans*-DCE (Fig. 5). The broadness of these bands is related to various desorption channels of acetylene generated from different adstructures as a result of annealing to different temperatures (Fig. 2b). In particular, the mass 26 TDS intensity over the 450–580 K region could be attributed to dechlorination of the mono-σ bonded chlorovinyl adspecies (Structures IV and V) to form a gaseous acetylene molecule that is released from the surface. The mass 26 TDS intensity found at 580–820 K could be assigned to acetylene released from the di-σ bonded vinylene adspecies (Structure VI, Fig. 2b) upon further annealing to these temperatures. It is of interest to note the TDS profiles of mass 26 ($C_2H_2^+$) for a saturation exposure of *cis*- and *trans*-DCE on an argon-sputtered Si(1 1 1) surface do not exhibit the broad intensity in the 450–580 K as found in those for the 7×7 surface (Figs. 4 and 5), which suggests that the sputtered Si surface is more reactive and tends to promote dissociation of the adspecies. It should be noted that we also monitored but found no desorption feature for mass 27, which belongs to the cracking pattern of and could therefore be used as a signature for ethylene (the parent mass of ethylene, mass 28, is not monitored due to high background).

In order to further investigate the nature of the surface products during thermal evolution, we record EELS spectra for 1000 L of *cis*-DCE (Fig. 6) and *trans*-DCE (Fig. 7) exposed to Si(1 1 1)7×7 at RT as a function of the annealing temperature. These temperature-dependent EELS spectra are found to be similar to each other for both *cis*- and *trans*-DCE, suggesting similar thermal evolution patterns for the adspecies of these adsorbates. In particular, upon annealing *cis*-DCE (Fig. 6b) or *trans*-DCE (Fig. 7b) on Si(1 1 1)7×7 to 450 K, we observe discernible strengthening in the Si–Cl stretch at 510 cm^{-1} and minor

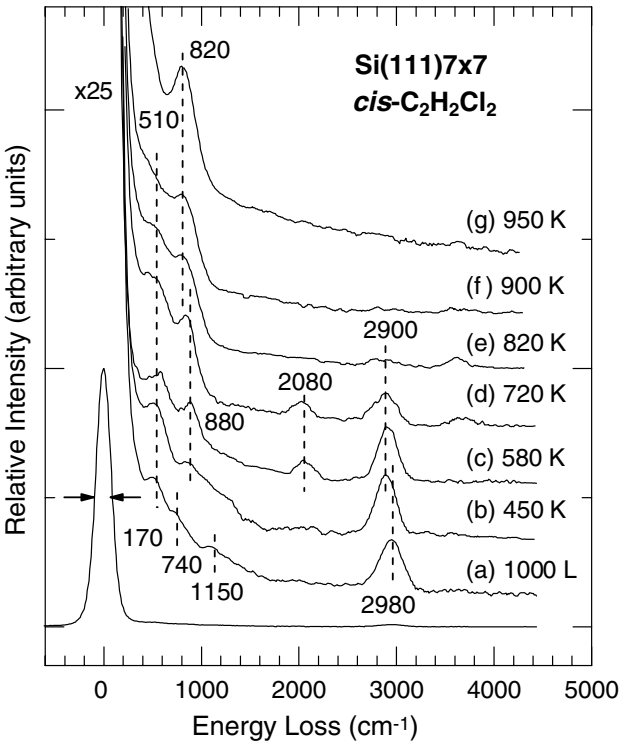

Fig. 6. Vibrational electron energy loss spectra for 1000 L of *cis*-dichloroethylene exposed to (a) Si(1 1 1)7×7 at room temperature, and upon annealing to (b) 450 K, (c) 580 K, (d) 720 K, (e) 820 K, (f) 900 K and (g) 950 K.

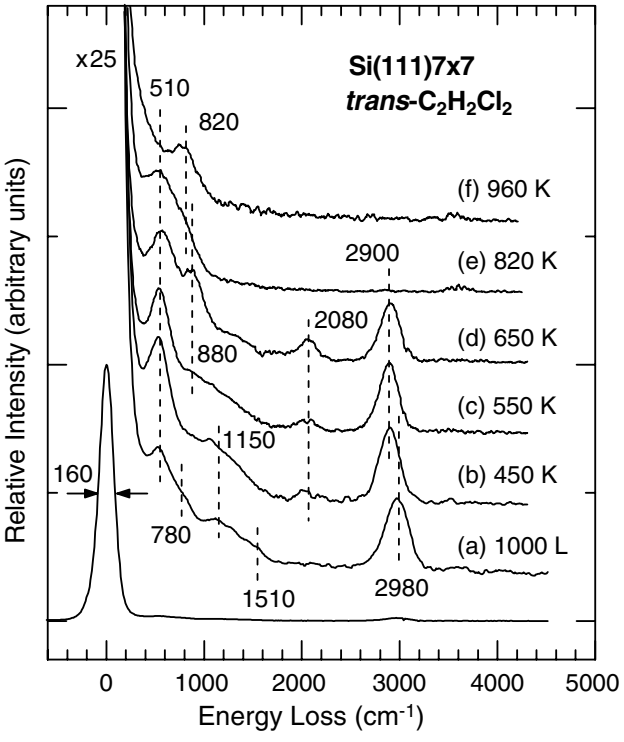

Fig. 7. Vibrational electron energy loss spectra for 1000 L of *trans*-dichloroethylene exposed to (a) Si(1 1 1)7×7 at room temperature, and upon annealing to (b) 450 K, (c) 550 K, (d) 650 K, (e) 820 K, and (f) 960 K.

weakening of the CH bending band with maximum at 1150 cm^{-1}, along with a red shift in the prominent C–H stretch feature at 2980–2900 cm^{-1}. The intensity of the Si–Cl stretch at 510 cm^{-1} is found to level off upon annealing to 550–580 K (Figs. 6c and 7c) and become totally diminished upon further annealing to above 900 K (Figs. 6f and 7f). This change is consistent with the thermal dechlorination of 2-chlorovinyl adspecies above 450 K (Fig. 2b) and the on-set of Cl removal channels above 580 K via recombinative desorption of HCl at 700–900 K and formation of $SiCl_2$ at 800–950 K as supported by our TDS data (Figs. 4 and 5). The CH bending modes in the 800–1400 cm^{-1} region are also found to be completely reduced upon annealing the samples above 580 K (Figs. 6c,d and 7c,d), which is consistent with our picture of total breakdown of the vinylene adspecies (Structure VI, Fig. 2b) to hydrocarbon fragments above 580 K. Furthermore, the observed red shift in the C–H stretch at 2980 cm^{-1} (Figs. 6a and 7a) to 2900 cm^{-1} upon annealing the samples to 450 K for *cis*-DCE (Fig. 6b) and *trans*-DCE (Fig. 7b) is consistent with our proposed thermal evolution pathway of 2-chlorovinyl adspecies (Structures IV and V) to vinylene (Structure VI) shown in Fig. 2b. In particular, in addition to the change in the C hybridization from sp^2 to sp^3, the red shift in the C–H stretch feature could also be caused by a change in the immediate chemical environment (i.e., the attached ligands or groups) of the host C atom. The C–H bond in the ($=C\langle^{H}_{Si}$) group as in vinylene (Structure VI, Fig. 2b) is slightly weaker than that in the ($=C\langle^{H}_{Cl}$) group as in 2-chlorovinyl adspecies (Structures IV and V, Fig. 2b) due to the lower electronegativity of Si (1.8 in the Pauling scale) relative to H (2.1) and C (2.5) [40]. It is of interest to note that the red shift in the C–H stretch at 2980 cm^{-1} has been observed in the thermal evolution of *iso*-DCE on Si(1 1 1)7 × 7 but at a slightly higher temperature than 450 K [24], which indicates that the presence of the pathway involving vinylidene (Structure II, Fig. 2a) appears to delay the on-set of the vinylene formation (with the characteristic red shift in the C–H stretch). For the annealing temperature from 450 K to ~700 K, the intensities of the red-shifted C–H stretch feature at 2900 cm^{-1} for the *cis*-DCE and *trans*-DCE samples are found to gradually reduced and become totally extinct upon further annealing to 820 K (Figs. 6b–e and 7b–e), which marks the completion of hydrogen abstraction and the formation of SiC.

In addition, three new features at 820 cm^{-1}, 880 cm^{-1} and 2080 cm^{-1} are observed at different annealing temperatures above 450 K for both *cis*-DCE and *trans*-DCE on Si(1 1 1)7 × 7. The new feature at 820 cm^{-1} that emerges above 820 K (Figs. 6e and 7e) and becomes a prominent well-defined peak above 950 K (Figs. 6g and 7f) can be assigned to the Si–C stretch. These spectral changes in the higher-temperature regime are in good accord with the breakdown of the hydrocarbon fragment adspecies and the formation of SiC above 820 K, as was commonly observed for other chlorinated ethylene adspecies in our recent studies [24,25]. In accord with the early work [30] and our recent study [24], the new features at 880 cm^{-1} and 2080 cm^{-1} could be primarily attributable to the SiH_2 scissoring and Si–H stretching modes, respectively. It should be noted that the SiH_2 scissoring mode at 880 cm^{-1} can be used to indicate the presence of dihydrides while the broad Si–H band at 2080 cm^{-1} cover contributions from both dihydrides and monohydrides. Discernible intensities of these features are found at an annealing temperature near 550 K (Figs. 6c and 7c) and appear to increase at 650–720 K (Figs. 6d and 7d), which marks the on-set of hydrogen abstraction of the adspecies onto the surface and the formation of hydrocarbon fragments, likely in the form of CCH radicals with characteristic CH bending modes at 850–900 cm^{-1} [14]. Furthermore, these features at 880 cm^{-1} and 2080 cm^{-1} become totally diminished above an annealing temperature of 820 K (Figs. 6e and 7e), which is consistent with the recombinative desorption of H_2 from dihydrides at 600–750 K and monohydrides at 700–820 K and of HCl at 700–900 K as observed in our TDS experiments (Figs. 4 and 5). It should be noted that the weak OH stretch feature near 3600 cm^{-1} found in Figs. 6d–f and 7e,f could be attributed to minor water contamination during the long time required for sample recooling to RT before the EELS spectra were recorded.

Although the overall change for *trans*-DCE during thermal annealing is similar to that for *cis*-DCE, there are some notable differences. In particular, a broad feature near 900 cm^{-1} is clearly observed in the *cis*-DCE spectrum (Fig. 6b) but not the *trans*-DCE spectrum (Fig. 7b) after the 450 K anneal. Given that both the SiH_2 scissoring mode and the CCH bending modes of the vinylene adspecies may contribute to the broad feature at 900 cm^{-1}, the presence of this weak feature in the *cis*-DCE spectrum but not the *trans*-DCE spectrum therefore suggests that thermal evolution of the 2-chlorovinyl conformer for *cis*-DCE (Structure IV, Fig. 2b) to the di-σ bonded vinylene (Structure VI, Fig. 2b) occurs at a lower temperature than that for *trans*-DCE (Structure V, Fig. 2b). Such a difference may be related to the different conformations for the mono-σ bonded 2-chlorovinyl adspecies, which provide different proximities of the Cl atom to the surface. Another discernible difference is the stronger relative intensity of the Si–Cl feature at 510 cm^{-1} over the desorption temperature range of 450–820 K for the *trans*-DCE sample (Fig. 7b–e) than that for the *cis*-DCE sample (Fig. 6b–e). For example, the intensity ratio for the Si–Cl feature at 510 cm^{-1} relative to the C–H stretch at 2900 cm^{-1} at 450 K for *trans*-DCE (Fig. 7b) is estimated to be 1.2, which is larger than the corresponding intensity ratio at 450 K for *cis*-DCE (0.7, Fig. 6b). The notable difference is therefore not due to run-to-run variations in our EELS experiments. This difference is in good accord with our TDS data and could be caused by different steric effects exerted by the geometrical isomers in the initial adsorption/dechlorination process.

3.3. Feasibility of vinylidene and vinylene on Si(1 1 1)7 × 7

To further investigate the feasibility of the formation of vinylidene and vinylene on the 7 × 7 surface, we perform ab initio density functional calculations for selected adsorption structures for *iso*-DCE, *cis*-DCE and *trans*-DCE on the surface of a Si_9H_{12} cluster, used for simulating part of the Si(1 1 1)7 × 7 surface [41]. The hybrid functionals consisting of Becke's 3-parameter non-local exchange functional and the correlation functional of Lee–Yang–Parr (B3LYP) [42] along with the 6-31G(d) basis set are employed in our calculations using the Gaussian 03 program [43]. The Si_9H_{12} cluster is constructed to provide a small section of the simulated 7 × 7 surface that contains a corner adatom and a neighbouring restatom, using the geometry parameters for the Si atoms deduced from the LEED data of Tong et al. [44]. In this dimer adatom stacking-fault model of the 7 × 7 surface, the separation between an adatom and a restatom and that between an adatom and a pedestal atom are 4.6 Å and 2.4 Å, respectively [44]. Following the approaches used by Wang et al. [41] and Petsalakis et al. [45], we first optimize the positions of the H atoms used to cap the cluster at the boundaries with the nine Si atoms frozen at the coordinates provided by Tong et al. [44]. The optimized positions of the H atoms are then frozen to provide an effective cage to maintain the structure of the model surface for the subsequent calculations, in which only the positions of the nine Si atoms and the atoms in the adsorbate are allowed to be optimized. It is important to note that the present calculations are only intended to illustrate some of the structures proposed in the thermal evolution pathways shown in Fig. 2. More extensive calculations that cover many other combinations of different bonding sites on the 7 × 7 surface should be considered to provide a more complete picture in future computational work. The use of a larger basis set, however, is not expected to significantly change the general observations inferred from the present calculations.

Fig. 8 shows some of the plausible adstructures involving di-σ bonded [2 + 2] cycloaddition species (top row), mono-σ bonded dissociated products (second row), and double-dissociation products involving di-σ bonding between the adatom and the pedestal atom (bottom three rows). Except for the di-σ bonded [2 + 2] cycloaddition products, we have also determined the related (less stable) conformer adstructures, obtained by transposition of the dissociated Cl atom with the chlorovinyl fragment in A2, B2 and C2 (Fig. 8) and with the dissociated H atom in A3, B4, C3, and C4 (Fig. 8). Two conformers for vinylidene-related adstructures of *iso*-DCE (A4 and A4′) and for vinylene-related adstructures of *cis*-DCE (B3 and B3′) are also shown in Fig. 8. The corresponding total-energy changes with zero-point energy corrections, ΔH, for the adstructures and the aforementioned conformer adstructures (values shown in parentheses) are also included in Fig. 8. The magnitudes of the energy differences among different ΔH values obtained for the di-σ bonded molecular adstructures, mono-σ bonded dissociated chlorovinyl adstructures, and the double-dissociation adstructures involving di-σ bonding into the back-bond (vinylidene and vinylene and their chlorinated derivatives) are evidently related to the energy balances involved in the breakage of the C–Cl (with a typical bond energy ΔH_B of 339 kJ mol^{-1}) and C–H bonds ($\Delta H_B = 414$ kJ mol^{-1}) and the formation of the Si–Cl ($\Delta H_B = 377$ kJ mol^{-1}), Si–C ($\Delta H_B = 347$ kJ mol^{-1}) and Si–H bonds ($\Delta H_B = 314$ kJ mol^{-1}) [1,31,32]. Evidently, the di-σ bonded [2 + 2] cycloaddition products (A1, B1, C1) are considerably less thermodynamically favourable (with the least negative ΔH values) than the dissociated adstructures, in good accord with our experimental observations. Furthermore, the ΔH values obtained for the adspecies involving double dechlorination (A4′, B3′) are more negative than those involving dehydrochlorination (i.e., single dechlorination and single H abstraction) (A3, B4, C3, C4) and those involving just single dechlorination (A2, B2, C2), which are in turn more negative than those involving double dehydrogenation (A4, B3). In particular, the ΔH value obtained for double dechlorination of *iso*-DCE involving insertion of a vinylidene adspecies into the back-bond between an adatom and a pedestal atom (A4′ with $\Delta H = -510.2$ kJ mol^{-1}) is the most negative, which suggests that vinylidene is physically viable through the breakage of the back-bond and appears to be the most thermodynamically stable adspecies for *iso*-DCE [24]. On the other hand, dehydrochlorination of *cis*-DCE involving insertion of a chlorovinylidene adspecies (a chlorinated derivative of vinylidene) into the back-bond (B4 with $\Delta H = -382.9$ kJ mol^{-1}) is found to be less thermodynamically favourable than double dechlorination involving insertion of vinylene into the back-bond (B3′ with $\Delta H = -478.4$ kJ mol^{-1}). In the case of *trans*-DCE, the latter adstructure involving vinylene insertion into the back-bond for *cis*-DCE (i.e., B3′) could also be made viable by an intermediate step involving sequential Cl abstraction and the formation of acetylene-like intermediate adspecies. The formation of the dehydrochlorination adstructure involving insertion of chlorovinylene into the back-bond for *trans*-DCE (C3 with $\Delta H = -349.3$ kJ mol^{-1}) is also found to be less thermodynamically favourable than that of the double-dechlorination vinylene adstructure (B3′ with $\Delta H = -478.4$ kJ mol^{-1}). Unlike the chlorovinylidene adstructures (B4 with $\Delta H = -382.9$ kJ mol^{-1} and C4 with $\Delta H = -394.3$ kJ mol^{-1}), the formation of the vinylene adstructure (B3′) is more compatible with the evolution from the single-dechlorination adstructures involving 2-chlorovinyl adspecies, B2 for *cis*-DCE and C2 for *trans*-DCE (Fig. 8), as depicted in Fig. 2b.

In Fig. 9, we compare selected adstructures of the double-dissociation products involving insertion into the back-bond (A3, B3, B3′ and C3) in Fig. 8 with the same products di-σ bonded to an adatom–restatom pair (similar to the [2 + 2] cycloaddition adstructures). For the latter adstructures, the corresponding ΔH values are estimated

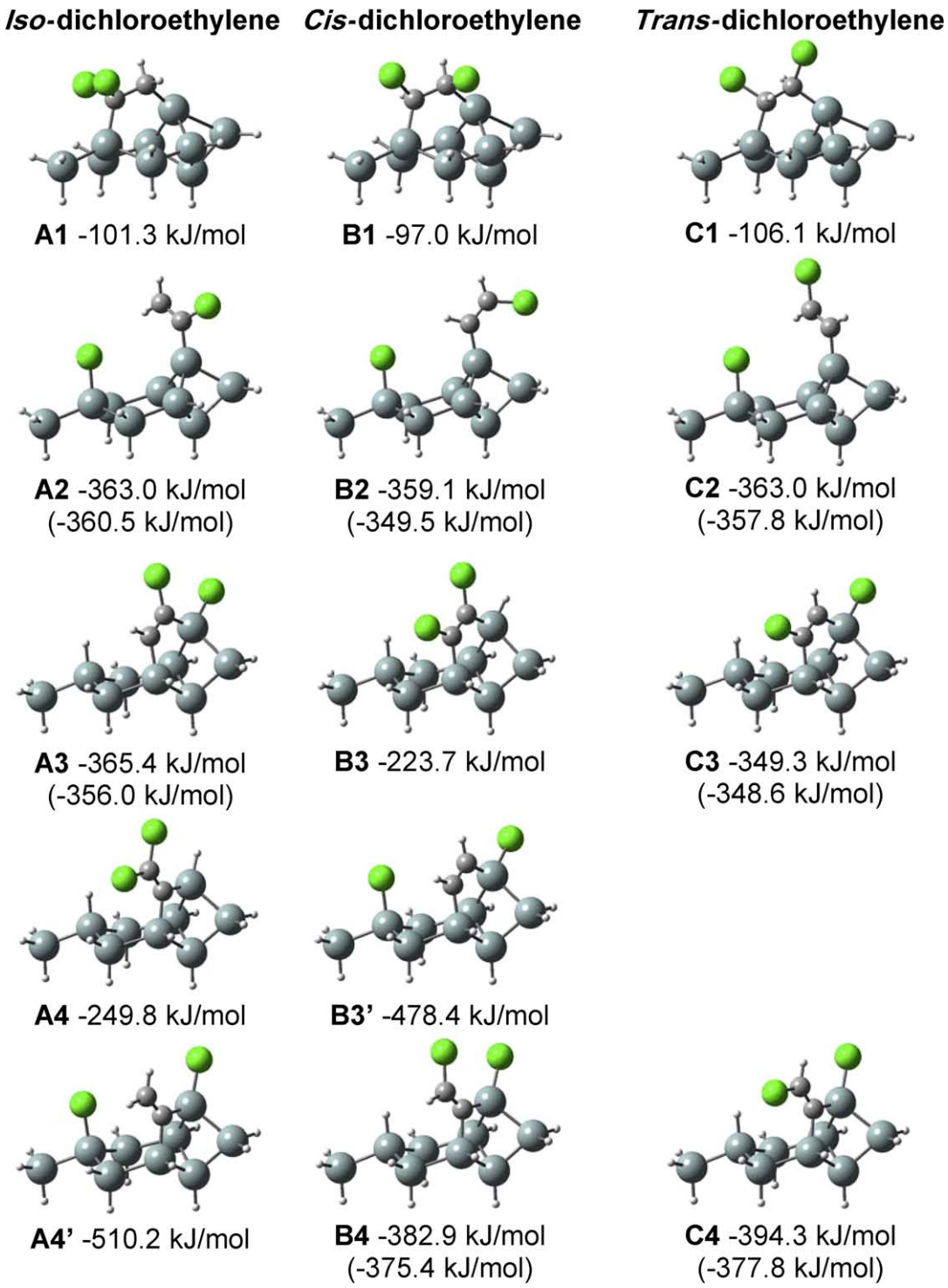

Fig. 8. Adsorption geometries and adsorption energies ΔH of selected adstructures obtained by density functional calculations involving B3LYP/6-31-G(d) for (A) *iso*-dichloroethylene, (B) *cis*-dichloroethylene, and (C) *trans*-dichloroethylene on a model surface of Si_9H_{12}. The ΔH values of related conformer structures obtained by transposition of the dissociated atoms are given in parentheses.

by considering the changes in the total energies (with zero-point energy corrections) of the chlorohydrocarbon adspecies on a Si_9H_{12} cluster and of the dissociated Cl and/or H atoms on a second Si_9H_{12} cluster. The ΔH values for the conformer adstructures involving transposition of the dissociated Cl and H atoms on the second Si_9H_{12} cluster for A5 and C5 are indicated in parentheses in Fig. 9. It should be noted that the geometry for the Si_9H_{12} cluster for these latter adstructures (A5, B5, B5′ and C5) is very similar to that found for the [2 + 2] cycloaddition adstructures (A1, B1 and C1 in Fig. 8). However, the bond lengths of the back-bonds of the adatom (2.8–2.9 Å) [and restatom

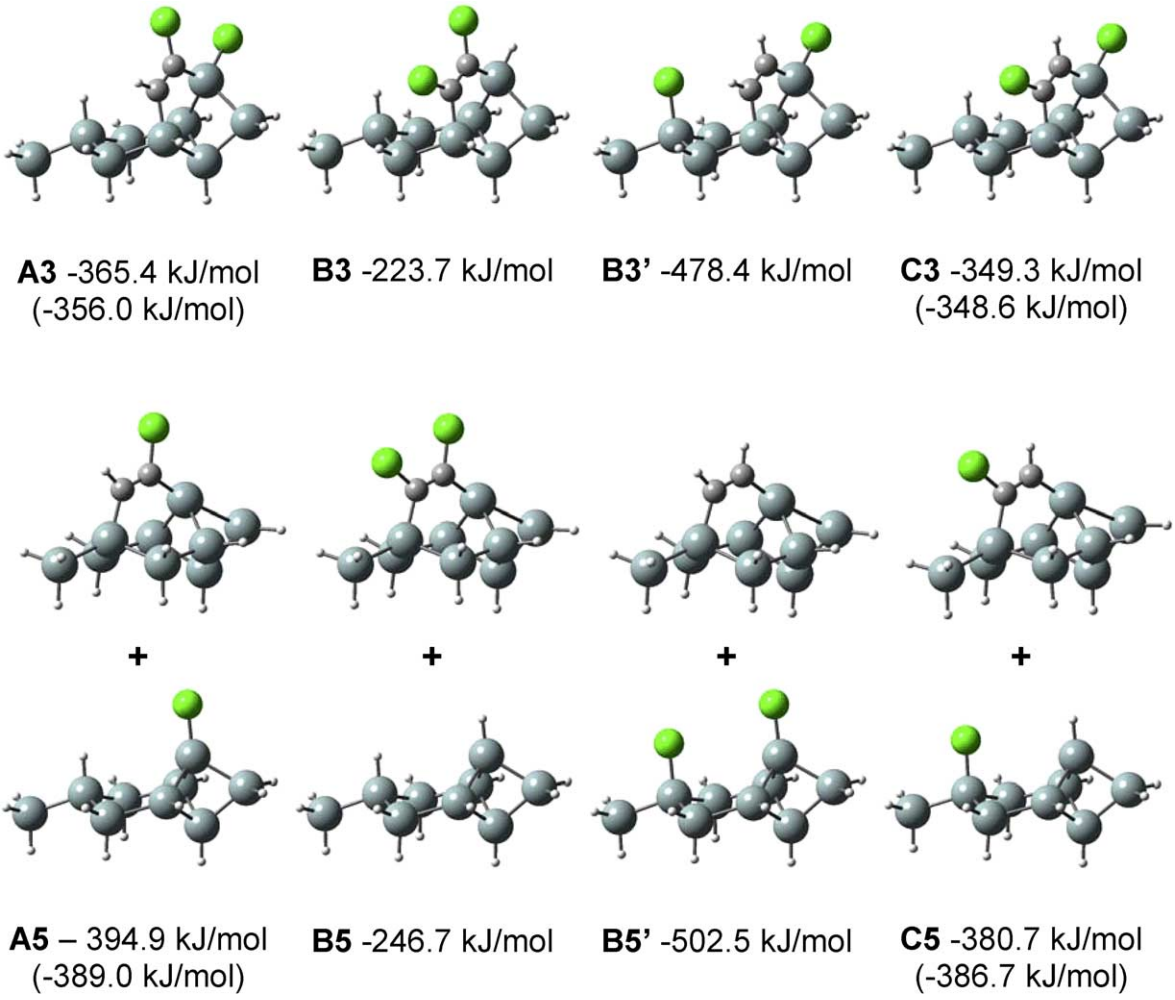

Fig. 9. Comparison of the adsorption geometries and adsorption energies ΔH of selected adstructures of double-dissociation products involving insertion into the back-bond (A3, B3, B3′ and C3 in Fig. 8) with those involving di-σ bonding to an adatom–restatom pair (A5, B5, B5′ and C5). The adsorption geometries and ΔH are obtained by density functional calculations involving B3LYP/6-31-G(d) on a model surface of Si_9H_{12}. The ΔH values of related conformer structures obtained by transposition of the dissociated atoms are given in parentheses.

(2.4–2.5 Å)] upon the addition of the (chloro)vinylene adspecies are found to be discernibly longer than that of the pristine surface, i.e., without the adspecies (2.3–2.4 Å). These bond lengths are however shorter than the separations between the adatom and the pedestal atom in the A3, B3, B3′ and C3 adstructures (3.3–3.4 Å), in which the back-bonds are considered to be broken. As evidenced from the slightly more negative ΔH values for the A5, B5, B5′ and C5 adstructures than the corresponding A3, B3, B3′ and C3 adstructures shown in Fig. 9, insertion of the (chloro)vinylene adspecies into the adatom–restatom pair appears to be more thermodynamically favourable than insertion of the corresponding adstructure into the back-bond. Unlike vinylidene and its chlorinated derivatives that favour insertion into the back-bond (A4′, B4 and C4 in Fig. 8), vinylene and its chlorinated derivatives favour di-σ bonding between the adatom and the restatom (A5, B5, B5′ and C5 in Fig. 9). Using a typical Si–C bond length of 1.9 Å [46] and a bond angle between C=C and Si–C of 121°, the required separation for the two Si atoms is estimated to be 3.3 Å, which is more compatible with the larger Si-Si separation between an adatom and a neighbouring restatom (4.6 Å) than the smaller separation between an adatom and its pedestal atom (2.4 Å) that would require the breakage of the back-bond [19,24].

It should be noted although the calculated ΔH values for all the adstructures shown in Figs. 8 and 9 are negative, the present calculations have not considered kinetic effects. The present results should therefore only be used to indicate their thermodynamic feasibility. For example, in spite of having the least negative ΔH value, the [2 + 2] cycloaddition product is generally accepted to be the preferred adstructure for ethylene on Si(1 1 1)7 × 7 [17]. For the three geometrical isomers of DCE, our EELS and TDS data are more consistent with the proposed dissociation surface products, which suggests that their corresponding adstructures are more critically controlled by their thermodynamic stabilities as illustrated by the ΔH values estimated in the present calculations.

4. Summary

The effects of different geometrical isomeric structures on the RT adsorption and thermal evolution of *iso*, *cis*- and *trans*-DCE on Si(1 1 1)7 × 7 have been investigated by vibrational EELS and TDS, as well as density functional calculations. Both *cis*- and *trans*-DCE exhibit similar RT adsorption properties, which are notably different from *iso*-DCE. In particular, the presence of the Si–Cl feature at 510 cm^{-1} for all three isomers indicates that all three adsorbates undergo dechlorination on Si(1 1 1)7 × 7 upon adsorption at RT. The lower saturation exposure observed for *iso*-DCE than the *cis* and *trans* isomers suggests that Cl dissociation via the $=CCl_2$ group as in *iso*-DCE occurs more readily than the =CHCl group as in the *cis* and *trans* isomers, in accord with the earlier observation for C–Cl bond cleavage in multiply chlorinated hydrocarbons on metal surfaces [12]. It should be noted that for *cis*-DCE adsorbed on Cu(1 0 0), the corresponding TDS data obtained by Yang et al. [12] suggests that once the first C–Cl bond breakage occurs (at 185 K), the second C–Cl bond cleavage could follow promptly. This preference of double dechlorination on metal surfaces over single dechlorination is different from the behaviour of *cis*- and *trans*-DCE on Si(1 1 1)7 × 7 surface at RT (Structures IV and V, Fig. 2b), which could be related to the nature of directional surface dangling bonds of the 7 × 7 surface. For *iso*-DCE, further dechlorination via insertion of vinylidene into the back-bond (Structure II, Fig. 2a) is found to be plausible [24]. The presence of the TDS feature near 360 K attributable to molecular desorption suggests that, in addition to the dechlorination adstructures, molecular adstructures also exist upon the initial adsorption of all three isomers on the 7 × 7 surface at RT. This molecular adsorption may also serve as the precursor step to the aforementioned dissociative chemisorption through dechlorination.

Despite the minor differences in the adsorption properties between *iso*-DCE and its *cis*- and *trans* isomers, thermal evolution of the respective adstructures for all three isomers on Si(1 1 1)7 × 7 are found to be remarkably similar to one another (Fig. 2). In particular, the commonly observed mono-σ bonded chlorovinyl ($H\dot{C}{=}\dot{C}HCl$) adspecies (Structures I, IV and V, Fig. 2) is found, upon annealing to 450 K, to undergo further dechlorination to either vinylene di-σ bonded to the Si surface (Structures III and VI, Fig. 2) or acetylene to be released from the surface. Upon annealing the sample above 580 K, the di-σ bonded vinylene could also become acetylene to be released from the surface or undergo H abstraction to produce hydrocarbon or SiC fragments. Furthermore, our TDS data show not only substrate etching involving the production of $SiCl_2$ at an annealing temperature of 800–950 K, but also recombinative desorption of HCl and H_2 over the annealing temperature ranges of 700–900 K and 650–820 K, respectively. Although the overall change for the *trans*-DCE products during thermal annealing is similar to the case of *cis*-DCE, there are some discernible differences. In particular, the Cl-derived TDS signals and Si–Cl stretch feature at 510 cm^{-1} over the desorption temperature of 450–820 K for *trans*-DCE are found to be more intense than those for *cis*-DCE, which indicates stronger dechlorination for *trans*-DCE than *cis*-DCE. This difference is likely due to less steric hindrance resulting from the formation of the 2-chlorovinyl adspecies for *trans*-DCE during the initial adsorption/dechlorination process. Finally, our density functional calculations qualitatively support the thermodynamic feasibility and relative stabilities of the proposed adstructures involving chlorovinyl, vinylidene, and vinylene adspecies.

Acknowledgement

This work was supported by the Natural Sciences and Engineering Research Council of Canada.

References

[1] J.M. Buriak, Chem. Rev. 102 (2002) 1271.
[2] V.G. Lifshits, A.A. Saramin, A.V. Zotov, Surface Phases on Silicon, Wiley, New York, 1994.
[3] R. Kuster, K. Christmann, Ber. Bunsen-Ges. 101 (1997) 1799.
[4] Q.A. Huang, J.N. Chen, H.Z. Zhang, Q.Y. Tong, Jpn. J. Appl. Phys., Part 1 32 (1993) 2854.
[5] A.K Hochberg, A. Lagendijk, D.A. Roberts, R. Agny, B. Anders, R. Cotner, J. Jewett, J. Mulready, M. Tran, B.B. Triplett, P. Werner, J. Electrochem. Soc. 139 (1992) L117.
[6] I.W. Boyd, R.B. Jackman, Photochemical Processing of Electronic Materials, second ed., Academic, London, 1992.
[7] W. Sesselmann, T.J. Chuang, J. Vac. Sci. Technol. B3 (1985) 162.
[8] X.H. Chen, J.C. Polanyi, D. Rogers, Surf. Sci. 376 (1997) 77.
[9] Y. Cao, J.F. Deng, G.Q. Xu, J. Chem. Phys. 112 (2000) 4795.
[10] G.A. Somorjai, Introduction to Surface Chemistry and Catalysis, Wiley, New York, 1994.
[11] V.H. Grassian, G.C. Pimental, J. Chem. Phys. 88 (1988) 4478.
[12] M.X. Yang, P.W. Kash, D.-H. Sun, G.W. Flynn, B.E. Bent, M.T. Holbrook, S.R. Bare, D.A. Fischer, J.L. Gland, Surf. Sci. 380 (1997) 151.
[13] Y. Jugnet, N.S. Prakash, J.C. Bertolini, S.C. Laroze, R. Raval, Catal. Lett. 56 (1998) 17.
[14] S.C. Laroze, S. Haq, R. Raval, Y. Jugnet, J.C. Bertolini, Surf. Sci. 433–435 (1999) 193.
[15] L.H. Bloxham, S. Haq, C. Mitchell, R. Raval, Surf. Sci. 489 (2001) 1.
[16] A. Cassuto, M.B. Hugenschmidt, Ph. Parent, C. Laffon, H.G. Tourillon, Suf. Sci. 310 (1994) 390.
[17] J. Yoshinobu, H. Tsuda, M. Onchi, M. Nishijima, Chem. Phys. Lett. 130 (1986) 170.
[18] J. Yoshinobu, H. Tsuda, M. Onchi, M. Nishijima, Solid State Commun. 60 (1986) 801.
[19] C. Huang, W. Widdra, X.S. Wang, W.H. Weinberg, J. Vac. Sci. Technol. A 11 (1993) 2250, and references therein.
[20] F. Rochet, F. Jolly, F. Bournel, G. Dufour, F. Sirotti, J.-L. Cantin, Phys. Rev. B 58 (1998) 11029.
[21] V. De Renzi, R. Biagi, U. del Pennino, Phys. Rev. B 64 (2001) 155305.
[22] Z.H. He, X. Yang, X.J. Zhou, K.T. Leung, Surf. Sci. 547 (2003) L840.
[23] X.J. Zhou, Q. Li, Z.H. He, X. Yang, K.T. Leung, Surf. Sci. 543 (2003) L668.
[24] Z.H. He, Q. Li, K.T. Leung, J. Phys. Chem. B 109 (2005) 14908.
[25] Z.H. He, K.T. Leung, Surf. Sci. 583 (2005) 179.
[26] D.Q. Hu, Ph.D. thesis, University of Waterloo, Waterloo, 1993.
[27] T. Shimanouchi, Tables of Molecular Vibrational Frequencies, Consolidated Vol. I, National Bureau of Standards, 1972, p. 1.

[28] J. Schmidt, C. Stuhlmann, H. Ibach, Surf. Sci. 302 (1994) 10.
[29] Q. Gao, C.C. Cheng, P.J. Chen, W.J. Choyke, J.T. Yates Jr., J. Chem. Phys. 98 (1993) 8308.
[30] H. Ibach, D.L. Mills, Electron Energy Loss Spectroscopy and Surface Vibrations, Academic, New York, 1982.
[31] R.T. Sanderson, Polar Covalence, Academic, New York, 1983.
[32] R.T. Sanderson, Chemical Bonds and Bond Energy, second ed., Academic, New York, 1976.
[33] M.X. Yang, S. Sarkar, B.E. Bent, S.R. Bare, M.T. Holbrook, Langmuir 13 (1997) 229.
[34] Eight Peak Index of Mass Spectra, vol. 1, Mass Spectrometry Data Center, Aldermaston, 1974.
[35] P.A. Coon, P. Gupta, M.L. Wise, S.M. George, J. Vac. Sci. Technol. A 10 (1992) 324.
[36] D.D. Koleske, S.M. Gates, D.B. Beach, J. Appl. Phys. 72 (1992) 4073.
[37] K.H. Junker, G. Hess, J.G. Eherdt, J.M. White, J. Vac. Sci. Technol. A 16 (1998) 2995.
[38] K. Oura, V.G. Lifshits, A.A. Saranin, A.V. Zotov, M. Katayama, Surf. Sci. Rep. 35 (1999) 1.
[39] R.M. Wallace, P.A. Taylor, W.J. Choyke, J.T. Yates, Surf. Sci. 239 (1990) 1.
[40] D.R. Lide (Ed.), CRC Handbook of Chemistry and Physics, 85th ed., CRC Press, Boca Raton, 2005.
[41] Z.H. Wang, Y. Cao, G.Q. Xu, Chem. Phys. Lett. 338 (2001) 7.
[42] J.B. Foresman, Æ. Frisch, Exploring Chemistry with Electronic Structure Methods, second ed., Gaussian Inc., Pittsburgh, 1996, and references therein.
[43] M.J. Frisch et al., Gaussian 03, Revision B.04, Gaussian, Inc., Pittsburgh, PA, 2003.
[44] S.Y. Tong, H. Huang, C.M. Wei, W.E. Pachard, F.K. Men, G. Glander, M.B. Webb, J. Vac. Sci. Technol. A 6 (1988) 615.
[45] I.D. Petsalakis, J.C. Polanyi, G. Theodorakopoulos, Surf. Sci. 544 (2003) 162.
[46] J.E. Huheey, Inorganic Chemistry, third ed., Harper and Row, New York, 1983.